

Magnetic chitosan-functionalized cobalt-NHC: Synthesis, characterization and catalytic activity toward Suzuki and Sonogashira cross-coupling reactions of aryl chlorides

Abdol R. Hajipour^{a,b,*}, Shaghayegh Sadeghi Malek^a

^a Pharmaceutical Research Laboratory, Department of Chemistry, Isfahan University of Technology, Isfahan, 8415683111, Iran

^b Department of Neuroscience, University of Wisconsin, Medical School, 1300 University Avenue, Madison, 53706-1532, WI, USA

ARTICLE INFO

Keywords:

Cobalt-N-Heterocyclic carbene catalyst
Sonogashira cross-coupling reaction
Suzuki cross-coupling reaction
Magnetic chitosan
Aryl chlorides

ABSTRACT

Aryl chlorides are one of the most stable and available electrophiles, however, their coupling with nucleophiles remains a challenge in organic synthesis. Herein, we prepared a Cobalt-NHC (N-Heterocyclic carbene) complex anchored on magnetic chitosan nanoparticles and assayed its catalytic activity for the reactions of substituted phenylboronic acid and also phenylacetylene with derivatives of aryl chlorides. These reactions are of great importance since they are employed for the synthesis of unsymmetrical diarylethynes and biphenyls, which belong to a prime class of building blocks. The synthesized nanocatalyst was found to be highly efficient in Suzuki and Sonogashira coupling in terms of their activity and recyclability in polyethylene glycol (PEG) as a green reaction media under conditions of temperatures (70 and 100 °C) and Co loading (3 and 6 mol%). To the best of our knowledge, this is the first attempt of using cobalt-NHC complex for catalyzing the abovementioned reactions. Moreover, replacing the earth-abundant Cobalt-based catalyst as an alternative to high cost palladium make this approach promising from sustainable chemistry view.

1. Introduction

The cross-coupling reactions have been well developed to prepare biphenyls and related compounds in the laboratory and on the industrial scale [1]. Now Suzuki and Sonogashira type coupling reactions have been used widely owing to their valuable products in organic synthesis [2]. Over the last few decades, cross-coupling reactions of substituted phenylacetylenes and phenylboronic acids with aryl halides has attracted much attention because these reactions construct unsymmetrical diarylethynes and biaryls which are vital structures in natural products, pharmaceuticals, and biologically important molecules [3]. Therefore, many successful catalytic systems have been designed to catalyze these kinds of reactions [4–10]. Generally, what most of the established catalytic systems have in common, is the employment of palladium considered as a powerful and versatile strategy in the synthesis of fine chemicals [11–15]. However, these catalysts suffer from drawbacks such as relative scarcity, high cost and toxicity [16,17]. Moreover, the latest generation of palladium catalysts rely on utilizing phosphine ligands [18] that are air sensitive and toxic [19]. Therefore, a wide range of ligands proposed for cross-coupling catalysts, which among them

N-Heterocyclic carbenes (NHCs) have attracted a great deal of attention due to their considerable properties such as moisture and air stability, variety of structures, and steric tunability [20,21]. Besides, these NHCs can serve as an alternative to phosphine ligands [22] because they have the same σ -donor and show a low π -acceptor ability [23] under metal coordination chemistry [24]. To this date, many successful homogenous Pd-NHC catalysts have been reported for cross-coupling reactions [2, 25–32]. According to Pd catalysts challenges, intense investigations have been undertaken to establish more earth-abundant and sustainable alternatives in these reactions. Among earth-abundant transition metals, cobalt with considerable properties such as low-cost, wide availability, and high reactivity has emerged as a very favorable alternative [33–35]. Regarding the Sonogashira and Suzuki cross-coupling reactions catalyzed by cobalt, numerous studies have been carried out [16,36–38]. But none of them evaluate Co-NHC catalyst which catalyzed cross-coupling of the derivatives of phenylacetylene and phenylboronic acids. As cited, the most NHC-based catalysts developed are homogeneous, that induce ligand contamination of the products and bear difficulties of separation and recycling from the reaction mixture. Therefore, Immobilization of the catalysts on solid supports is a strategy to overcome the

* Corresponding author at: Pharmaceutical Research Laboratory, Department of Chemistry, Isfahan University of Technology, Isfahan, 8415683111, Iran.
E-mail address: haji@cc.iut.ac.ir (A.R. Hajipour).

<https://doi.org/10.1016/j.mcat.2021.111573>

Received 6 February 2021; Received in revised form 6 April 2021; Accepted 8 April 2021

Available online 17 April 2021

2468-8231/© 2021 Published by Elsevier B.V.

disadvantages of homogenous catalysts such as leaching of metal species and recovery problems. Silica [39], polymer [40], and magnetic nanoparticles [16] (MNPs) have been used as support [41]. However, the reported polymer or silica-supported catalysts have active sites in the entire regions of the supports, which impede the diffusion of the reagents into the interior of the supports, resulting in a decrease in their catalytic activity and reaction rate [23]. Among various supports, magnetic nanoparticles (MNPs) [42,43] have been employed as a promising alternative, because of their low toxicity, biodegradability, and easy separation by an external magnetic field, with no other workup processes [44]. On the other hand, shielding of MNPs has been carried out to prevent oxidation and self-aggregation. Various protecting layer have been reported in which chitosan are promising biopolymer due to its conclusive properties such as biodegradability and cost effectiveness [45–48].

Although the reported catalytic systems were highly efficient, most of them employ environmentally non-benign solvents, expensive metal, high-temperature reaction conditions and limited substrate study. So we were encouraged to design a heterogeneous catalyst in which Cobalt-NHC immobilized on magnetic chitosan nanoparticles. The catalytic activity of the prepared catalyst was evaluated in cross-coupling of substituted phenylboronic acids and phenylacetylenes with aryl chlorides under mild conditions in PEG as a green, thermally stable and commercially available solvent. Indeed, conclusive properties such as simple preparation, and easy recover ability of the magnetic catalyst make this synthesized catalyst a promising candidate for examining it in other cross-coupling reactions. Besides, the ability of the synthesized catalyst to apply aryl chlorides in cited cross-coupling reactions is very advantageous because they are cheaper and commercially available than aryl iodides/bromides.

2. Experimental section

2.1. Catalyst preparation

2.1.1. Synthesis of (1-(3-chloro-2-hydroxypropyl)-3-methyl imidazolium chloride) ionic liquid ([mim]Cl)

A mixture of 0.1 mol hydrochloric acid (HCl, 37 %) and 50 mL ethanol was poured into a flask equipped with a dropping funnel and a reflux condenser. The flask was put in an oil bath with a magnetic stirring bar. 8 mL of *N*-methyl imidazole (0.1 mol) was slowly added to the flask over a period of 15 min. To avoid the formation of by-products, the pH of the solution was adjusted to 6 using excess HCl. Afterward, 10 mL of epichlorohydrin (0.12 mol) was added dropwise into the resultant aqueous solution at 5 °C under vigorous stirring. The temperature of the mixture was then raised to 45 °C. After stirring at 45 °C for 4 h, 1-(3-chloro-2-hydroxypropyl)-3-methyl imidazolium chloride, a viscous light yellow ionic liquid (IL), was obtained. The remaining water, ethanol, and epichlorohydrin were then removed by means of reduced pressure distillation. For further purification, the as-prepared IL was passed through a silica gel-G60 column and drying in vacuum at 60 °C. The product yield was about 90 % and, it was characterized by FT-IR, ¹H NMR, and ¹³C NMR analyses and summarized in the supporting information [49].

2.1.2. Synthesis of magnetic chitosan (MC)

In spite of various methods used for preparation of Fe₃O₄, coprecipitation as the most facile and straightforward approach was employed in this work [50]. In this regard, FeSO₄·7H₂O (5.2 mmol, 1.46 g) was first added to a round-bottom flask containing FeCl₃·6H₂O (7.4 mmol, 2 g) dissolved in 100 mL of distilled deionized water (DDI), followed by ultrasonic for 30 min to achieve a homogenous solution. Then, NH₄OH solution (as an alkaline precipitation agent) was added dropwise into the resultant solution until the pH reached 10 and a black precipitate formed, followed by stirring at 80 °C in a nitrogen atmosphere for about 2 h to complete the crystallization. After being cooled to ambient

temperature, the as-obtained precipitate was separated from the solution using an external magnetic bar, followed by washing several times with deionized water (DI) and ethanol, and drying in an oven at 50 °C. Subsequently, the surface modification of the magnetic nanoparticles (MNPs) was performed with chitosan to address the agglomeration of MNPs and also generate amine groups [34]. For this purpose, MNPs (0.236 g) and 2 mL of acetic acid solution were mixed accompanied by a mixture of DI (11 mL) and chitosan (0.472 g), and the resultant mixture was then stirred for 15 min. Sodium sulfate solution (20 % W/V) was dispersed in the as-obtained mixture and intensively stirred for 1 h at room temperature. Finally, the magnetic chitosan (MC) was separated from the solution using an external magnet, followed by washing with ethanol several times and drying at 70 °C.

2.1.3. Preparation of MC supported Cobalt-NHC (Co-NHC@MC)

The MC (1.5 g) was added to a solution of [mim]Cl (5 mL) and trimethylamine (Et₃N) (36 mmol, 5 mL) in 10 mL of tetrahydrofuran (THF). The resulting mixture was allowed to reflux overnight at 60 °C. The desired product (me-Im@MC) was collected using an external magnetic bar, followed by washing with THF several times to remove redundant, and drying in a vacuum oven at 50 °C. To attach the cobalt ions to the (me-Im@MC), 1.2 g of this compound was added to 0.5 g of Co(OAc)₂·4H₂O (2 mmol) together with 1 g of sodium carbonate (9 mmol) dissolved in 10 mL of ethanol. Afterward, the reaction mixture was refluxed and stirred for 16 h at 75 °C. The resulting complex was separated, washed several times with ethanol, and dried at room temperature to afford Co-NHC@MC as a brown solid. At the end, the solid was separated, washed with water, and dried at 50 °C. The detailed preparation steps are illustrated in Scheme 1.

2.2. Catalytic activity

2.2.1. General procedure for the Suzuki reaction

In a round-bottom flask containing a mixture of PEG (6 mL) as the solvent, a mixture of aryl halide (1.0 mmol), phenylboronic acid (1.2 mmol), K₂CO₃ (2.0 mmol), and the synthesized catalyst (3 mol%) were stirred at 70 °C. The reaction's progress was assessed by TLC (hexane/ethyl acetate, 80:20) and GC. After the completion of the reaction, the organic layer was washed with water (3 × 10 mL) and ethyl acetate (3 × 10 mL) and dried over anhydrous MgSO₄. The related products were purified using column chromatography (n-hexane/ethyl acetate, 5:1) and characterized by ¹H NMR and ¹³C NMR analyses and summarized in the supporting information.

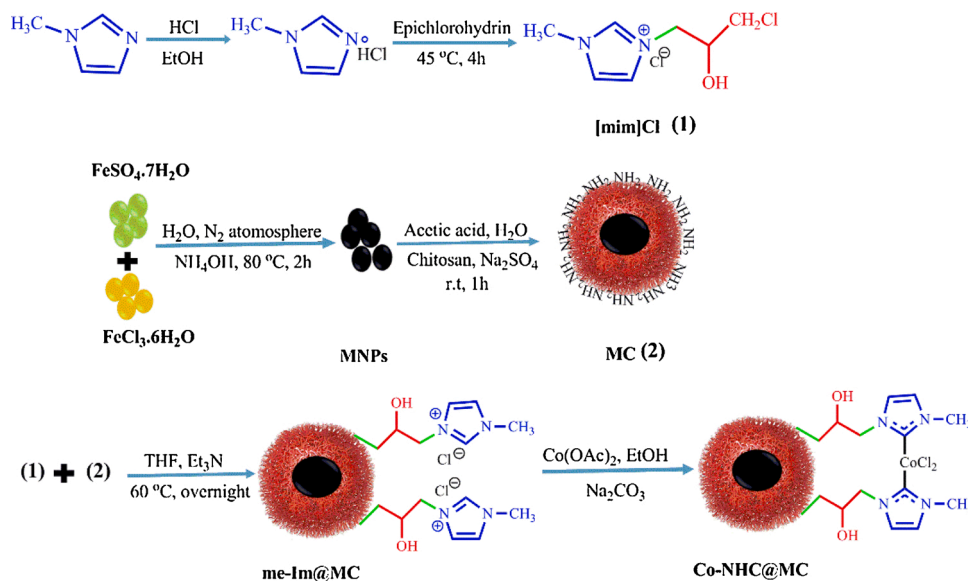
2.2.2. General procedure for the Sonogashira reaction

In a round-bottom flask containing a mixture of PEG (6 mL) as the solvent, a mixture of aryl halide (1.0 mmol), phenylacetylene (1.2 mmol), K₂CO₃ (2.0 mmol) and the catalyst (6 mol%) was added and the obtained mixture was stirred at 100 °C. The reaction was carried out similarly to the Suzuki reaction. The corresponding products were purified using column chromatography (n-hexane/ethyl acetate, 5:1) and characterized by ¹H NMR and ¹³C NMR analyses.

3. Results and discussion

3.1. Fabrication of Co-NHC@MC

To prepare Co-immobilization and -stabilization, magnetic chitosan (MC) were chosen as an appropriate support due to their magnetic properties, high surface to volume ratio, and convenient separation of the synthesized catalyst in combination with imidazolium chloride as the stabilizer. In recent years, many studies on the catalytic activity of imidazolium-based catalysts have been reported [51,52]. A schematic illustration has been designed (Scheme 1) to summarize the formation of the cobalt ion species on the me-Im@MC. The catalyst was prepared in 4 steps: in the first step, *N*-methyl imidazole reacted with epichlorohydrin



to form the imidazolium ionic liquid. Then, magnetic chitosan nanoparticles were synthesized and modified with imidazolium ionic liquid. Finally, $\text{Co}(\text{OAc})_2$ was used to form Co-NHC@MC. The amount of Co loading onto the catalyst was measured by inductively coupled plasma mass spectrometry analysis (3.94 mg L^{-1}).

3.2. Characterization of Co-NHC@MC

In order to prove the successful synthesizing of the catalyst, the FT-IR spectra of Fe_3O_4 , MC, [mim]Cl, and me-Im@MC, were obtained and shown in Fig. 1. The characteristic peaks for Fe_3O_4 can be seen in Fig. 1a. The bands at 3442 and 577 cm^{-1} are related to the stretching vibration of O—H and FeO—, respectively. In the case of magnetic chitosan, the absorption bands around 1081 , 1353 , 1583 and 3365 cm^{-1} are assigned to the stretching vibration of C—O, CN, NH— (primary amine) and OH—, respectively (Fig. 1b). In addition, the bands corresponding to the CH— (stretching vibration) of the chitosan backbone are appeared at 2921 and 2881 cm^{-1} (Fig. 1b). Fig. 1c illustrates the spectrum of the [mim]Cl where the bands for the C—Cl and OH— groups are found at 710 and 3400 cm^{-1} , respectively. The strong bands at 1635 and 1574 cm^{-1} correlated to the C=N and CC= vibrating bonds show the presence of imidazole group and also the bands in the range of 2850 to 2990 cm^{-1}

is related to the CH— sp^3 of the stretching vibration modes (symmetric and asymmetric) of the methylene groups. The band corresponding to the stretching vibrations of CO— group is appeared around 1000 – 1300 cm^{-1} (Fig. 1c). The spectrum of MC modified [mim]Cl is depicted in Fig. 1d. The disappearance of band at 710 cm^{-1} attributed to the CC—I group of imidazole ring and observed broaden bands in Fig. 1d in comparison with bands in Fig. 1c, indicate the successful attachment of imidazole groups to the magnetic chitosan.

X-ray photoelectron spectroscopy (XPS) as an effective method was utilized to clarify the binding of the cobalt-NHC and determine the valence states of the cobalt. The XPS experiment was performed for Co-NHC@MC and results are depicted in Fig. 2 (a–e). The XPS spectrum of Co 2p reveals two main peaks at 781.4 and 796.9 eV , indicating the binding energies of Co $2\text{p}_{3/2}$ and Co $2\text{p}_{1/2}$, respectively and suggests that the Co is in its two oxidation state (Fig. 2a) [53]. The two characteristic binding energy values of 196.48 and 199.38 eV are attributed to two spin-orbit pairs: Cl $2\text{p}_{3/2}$ and Cl $2\text{p}_{1/2}$, respectively (Fig. 2b). Moreover, the presence of Fe_3O_4 is confirmed by the two peaks at 710 and 724 eV , corresponded to Fe $2\text{p}_{3/2}$ and Fe $2\text{p}_{1/2}$, respectively (Fig. 2c). As observed in Fig. 2d, the status of carbon in Co-NHC@MC can be investigated by XPS spectrum of C1s. The C1s peak was deconvoluted into four peaks at 282.5 , 284.1 , 285.9 , and 288.3 eV , which are corresponded

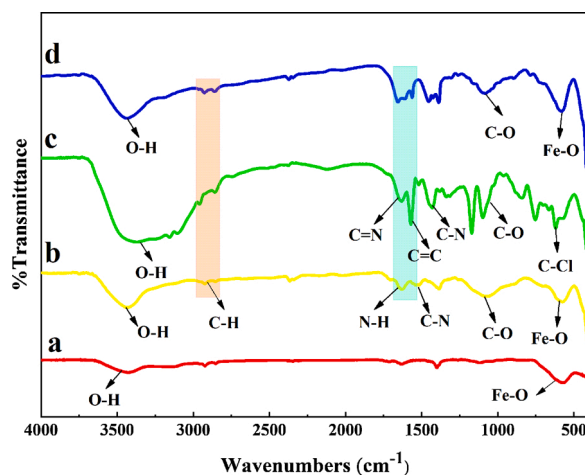


Fig. 1. FT-IR spectra: (a) Fe_3O_4 , (b) MC, (c) [mim]Cl, and (d) me-Im@MC.

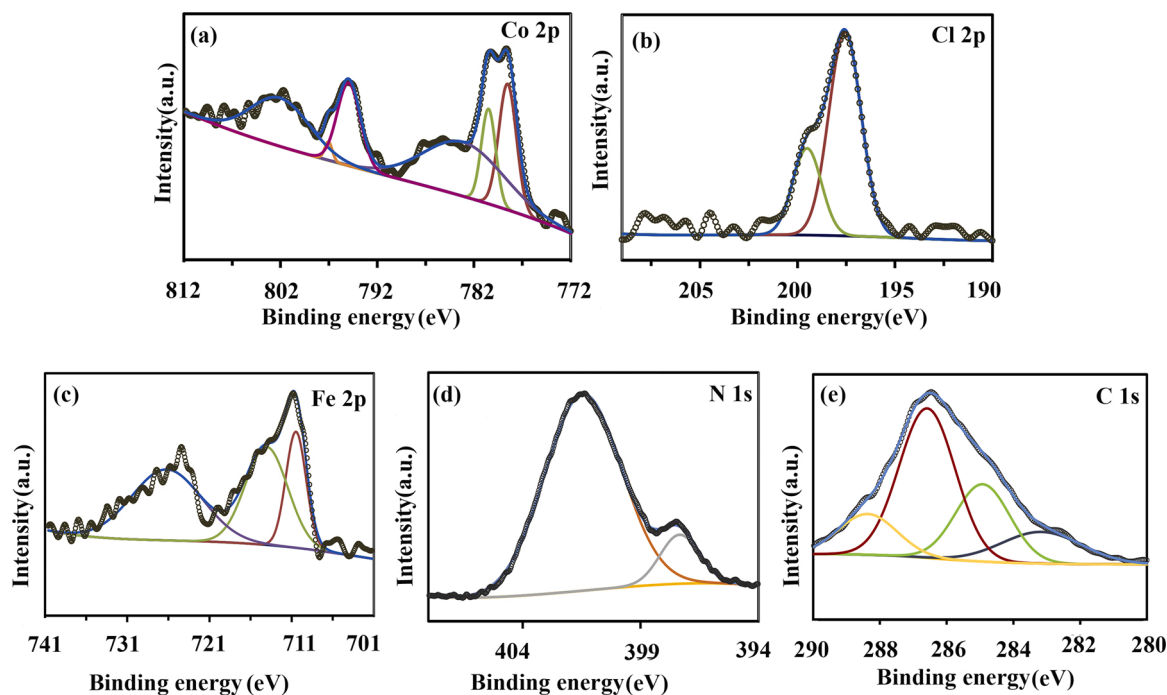


Fig. 2. XPS spectra of Co-NHC@MC (a-c) deconvoluted XPS spectra of Co 2p, Cl 2p, Fe 2p, C1s, and N1s, respectively.

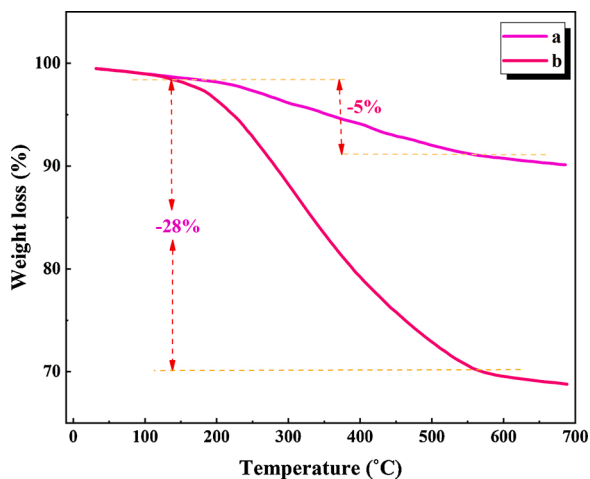


Fig. 3. TGA thermograms of (a) Fe_3O_4 (b) Co-NHC@MC.

to C=C, CC, CO—, and carbene. The N1s peaks appeared at 401.1 and 397.6 eV are related to N-sp²C and N-sp³C of aromatic ring of the NHC [54,55]. Therefore, the XPS-measurement confirms the successful synthesis of the Co-NHC@MC complex [56–58].

The thermal stability of the prepared catalyst was examined using thermogravimetric analysis (TGA). The TGA curve of Fe_3O_4 and Co-NHC@MC are shown in Fig. 3. A 5 wt% weight loss observed for Fe_3O_4 , is due to the removal of trapped water in magnetic nanoparticles' structure. However, for Co-NHC@MC weight loss steps observed is consequence of removal of adsorbed water and the decomposition of the organic backbone of catalyst. The total weight loss for Co-NHC@MC in the range of 150–550 °C is 28 %.

The presence of Fe_3O_4 and cobalt nanoparticles in the synthesized catalyst was explored by X-ray diffraction (XRD) analysis. Fig. 4 shows the XRD pattern of Fe_3O_4 and Co-NHC@MC samples. As observed in Fig. 4a, the six characteristic peaks at $2\theta = 30.2^\circ$, 35.6° , 43.3° , 53.8° , 57.4° , and 62.9° , can be related to crystal planes of Fe_3O_4 with cubic structure [59]. The XRD pattern of Co-NHC@MC reveals a broad peak at

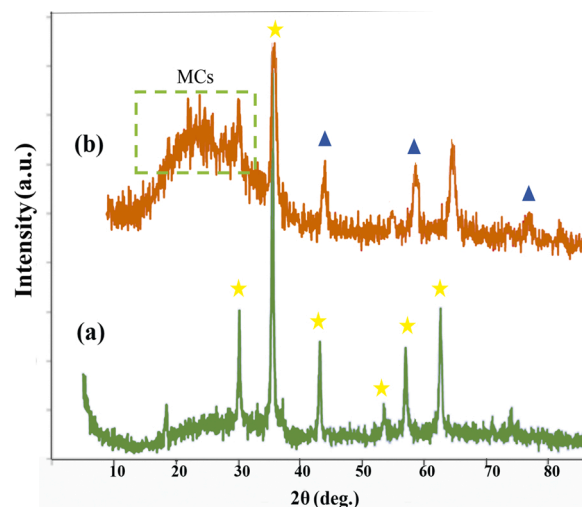


Fig. 4. XRD patterns of the (a) Fe_3O_4 , (b) Co-NHC@MC.

$2\theta = 20-30^\circ$ which indicate chitosan-coated magnetite nanoparticles [60]. The reduction in peaks intensity observed in XRD pattern of Co-NHC@MC confirms coating of magnetic nanoparticles by organic chains with an amorphous structure. As observed in Fig. 4b, the width of the peaks, as well as the peaks location, remained intact through the functionalization process, proving stability in structure of the nanoparticles. Moreover, the diffraction peaks observed at $2\theta = 43.2^\circ$, 56.5° , and 75.9° in Fig. 4b demonstrate the crystalline planes of the cobalt nanoparticle species with cubic spinel structure [61]. It is worthwhile to mention that the crystallographic phase of Fe_3O_4 nanoparticles is not affected by their surface modification (Fig. 4b). In addition, the average crystallite size of the nanoparticles estimated by the Scherrer equation was found to be 7.3 nm using the highest intensity peak (311).

The morphology evolution of synthesized catalyst is explored by field emission-scanning electron microscopy (FE-SEM). The outer topography of bare Fe_3O_4 and Co-NHC@MC are demonstrated in Fig. 5. As observed in Fig. 5a, the SEM image of Fe_3O_4 particles show uniform, regular and

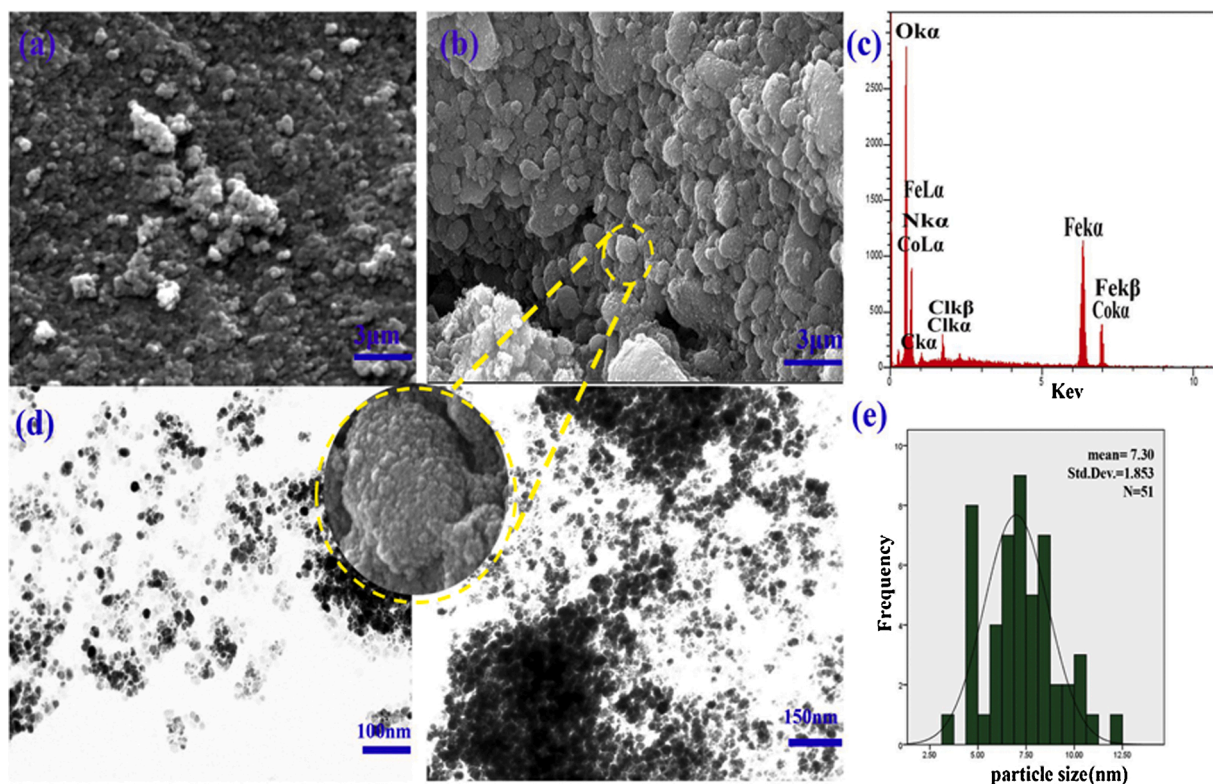


Fig. 5. FE-SEM images of (a) Fe₃O₄, (b) Co-NHC@MC, (c) SEM-EDX spectrum of the synthesized catalyst, (d) TEM images and (e) particle size distribution of Co-NHC@MC.

relatively aggregated surface. In comparison with the bare Fe₃O₄, the Co-NHC@MC show significant changes. On the one hand, the smooth surface is replaced with a rougher, coarse, and aggregated one. On the other hand, the average diameter is increased (Fig. 5b). Moreover, it is clearly seen the surface of Co-NHC@MC is coated with irregular nanoparticles. These results prove that the organic layer is grown on the surface of magnetic nanoparticles.

The chemical composition of Co-NHC@MC was further investigated by energy-dispersive X-ray (EDX) spectroscopy. Fig. 5c shows the significant peaks relating to elements of C, N, O, Fe, Cl and Co in the body of the catalyst. The internal structure of Co-NHC@MC is monitored using transmission electron microscopy (TEM) technique. The TEM images of Co-NHC@MC in Fig. 5d reveals the well-defined spherical shapes of the

nanoparticles, which include magnetic core/organic shell. Since the cobalt nanoparticles are smaller than the magnetic species, their presence is not detectable. According to the particle size distribution histogram, the average size of the catalyst was found to be 7.30 nm, which is in good agreement with XRD pattern results.

In order to explore the magnetic behavior of the Fe₃O₄ and synthesized catalyst, vibrating sample magnetometry (VSM) analysis was carried out and the magnetization curves are exhibited in Fig. 6. The magnetic saturation (M_s) value of Co-NHC@MC was decreased to 60

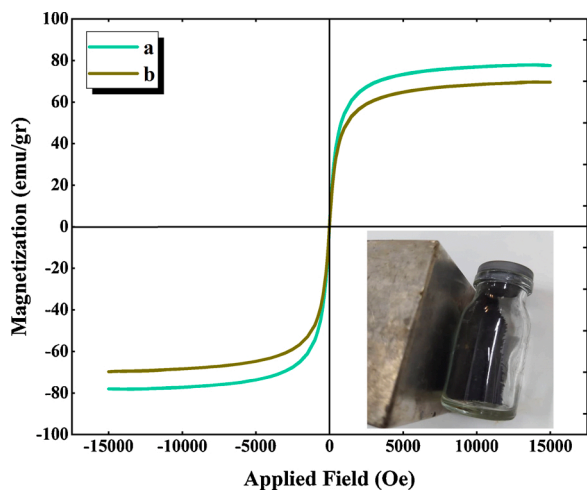


Fig. 6. Room temperature magnetization curves of (a) Fe₃O₄ and (b) the synthesized catalyst.

Table 1

Optimization of the reaction conditions in the Suzuki reaction of 1-chloro nitrobenzene and (4-methoxyphenyl) boronic acid in the presence of the catalyst.

Entry	Catalyst (mol %)	Base	Solvent	T (°C)/t (h)	Yield (%) ^a
1	–	K ₂ CO ₃	DMSO	90/24	–
2	Co-NHC@MC(5)	–	DMSO	90/24	–
3	Co-NHC@MC(5)	K ₂ CO ₃	DMSO	r.t./24	25
4	Co-NHC@MC(5)	K ₂ CO ₃	DMSO	90/10	97
5	Co-NHC@MC (5)	K ₂ CO ₃	DMF	90/10	96
6	Co-NHC@MC (5)	K ₂ CO ₃	NMP	90/10	84
7	Co-NHC@MC (5)	K ₂ CO ₃	PEG	90/10	95
8	Co-NHC@MC (5)	K ₂ CO ₃	PEG	90/8	94
9	Co-NHC@MC (5)	K ₂ CO ₃	PEG	90/5	81
10	Co-NHC@MC (5)	K ₂ CO ₃	PEG	70/10	93
11	Co-NHC@MC (5)	K ₂ CO ₃	PEG	70/8	92
12	Co-NHC@MC (5)	K ₂ CO ₃	PEG	50/8	68
13	Co-NHC@MC (5)	NaHCO ₃	PEG	70/8	79
14	Co-NHC@MC (5)	Na ₂ CO ₃	PEG	70/8	85
15	Co-NHC@MC (5)	Et ₃ N	PEG	70/8	72
16	Co-NHC@MC (5)	K ₃ PO ₄	PEG	70/8	77
17	Co-NHC@MC (4)	K ₂ CO ₃	PEG	70/8	89
18	Co-NHC@MC (3)	K₂CO₃	PEG	70/8	90
19	Co-NHC@MC (2)	K ₂ CO ₃	PEG	70/8	81

The optimum condition is exhibited in bold.

^a GC yield.

emu/gr compared with Fe₃O₄ (80 emu/gr) owing to covering of the surface of the magnetic nanoparticles with organic shell. However, the synthesized catalyst was still magnetic enough for efficient separation by an external magnetic field from the reaction mixture.

3.3. Application of the synthesized catalyst in C—C coupling reactions

After the characterization of the newly designed nanocomposite, the catalytic activity of the catalyst was studied in CC— bond formation via Suzuki and Sonogashira cross-coupling reactions.

3.3.1. Optimization of the reaction parameters for the Suzuki reaction

The effect of critical parameters such as the amount of catalyst, solvent, base and temperature on the reaction of 1-chloro-4-nitrobenzene with (4-methoxyphenyl) boronic acid as the model reaction was evaluated to achieve the optimal reaction conditions (Table 1). The effect of the solvent was the first parameter studied in the Suzuki cross-coupling reaction. Some common solvents were examined and it was also found that the yield achieved in the presence of PEG as the reaction media was almost as much as the ones obtained with other solvents. Temperature was the other parameter optimized in the Suzuki reaction. The reaction was evaluated at different temperatures, and the highest yield obtained at 70 °C. In the following step, various bases were

Table 2
Scope of the Suzuki cross-coupling reaction in the presence of the synthesized catalyst^a.

^bIsolated yield.

^a The reaction was carried out with aryl halide (1.0 mmol), phenylboronic acid (1.2 mmol), K₂CO₃ (2 mmol), in 6 mL PEG, and catalyst (3 mol% of Co) at 70 °C.

Table 3

Optimization of reaction conditions in the Sonogashira reaction of 1-chloro-4-nitrobenzene with 1-ethynyl-4-methoxybenzene in the presence of the catalyst.

Entry	Catalyst (mol %)	Base	Solvent	T (°C)/t (h)	Yield (%) ^a
1	–	K ₂ CO ₃	DMSO	120/24	–
2	Co-NHC@MC(10)	–	DMSO	120/24	–
3	Co-NHC@MC(10)	K ₂ CO ₃	DMSO	r.t./24	–
4	Co-NHC@MC(10)	K ₂ CO ₃	DMSO	120/15	91
5	Co-NHC@MC (10)	K ₂ CO ₃	DMF	120/15	89
6	Co-NHC@MC (10)	K ₂ CO ₃	NMP	120/15	76
7	Co-NHC@MC (10)	K ₂ CO ₃	PEG	120/15	89
8	Co-NHC@MC (10)	K ₂ CO ₃	PEG	120/10	89
9	Co-NHC@MC (10)	K ₂ CO ₃	PEG	120/8	81
10	Co-NHC@MC (10)	K ₂ CO ₃	PEG	100/10	86
11	Co-NHC@MC (10)	K ₂ CO ₃	PEG	80/10	68
12	Co-NHC@MC (10)	NaHCO ₃	PEG	100/10	73
13	Co-NHC@MC (10)	Na ₂ CO ₃	PEG	100/10	80
14	Co-NHC@MC (10)	Et ₃ N	PEG	100/10	69
15	Co-NHC@MC (10)	K ₃ PO ₄	PEG	100/10	75
16	Co-NHC@MC (8)	K ₂ CO ₃	PEG	100/10	85
17	Co-NHC@MC (6)	K₂CO₃	PEG	100/10	84
18	Co-NHC@MC (4)	K ₂ CO ₃	PEG	100/10	72

The optimum condition is exhibited in bold.

^a GC yield.

examined to achieve proper base. The base in the cross-coupling reaction plays an important role in neutralizing hydrogen halides and preventing the formation of homo-coupling products. The results reveal that among other bases, K₂CO₃ has the best performance. The amount of catalyst was the final parameter which was assayed in Suzuki reactions. As demonstrated in Table 1, The most proper amount of the catalyst in the Suzuki coupling reaction was 3 mol%. Additionally, the catalytic activity of the prepared catalyst in the Suzuki reaction was tested in the absence of the catalyst and no products were observed in this case.

3.3.2. Performance of the catalyst for the Suzuki reaction

To evaluate the catalytic activity of Co-NHC@MC, the Suzuki coupling reaction was conducted by derivatives of aryl chlorides and substituted phenylboronic acids in the presence of K₂CO₃ in PEG at 70 °C (Table 2). Although aryl chlorides are less reactive in cross-coupling reactions due to their strong bond dissociation, using them in cross-coupling is desirable owing to their accessibility and cost-effectiveness. And also, in comparison with aryl iodides and bromides more amount of catalyst and longer reaction time are needed to proceed the reaction. As exhibited in Table 2, the moderate to excellent yields were obtained for all substrates, and it was found that the reaction was sensitive to the nature of the functional groups (electron-donating or electron-withdrawing). It was clear that aryl chlorides, including electron-withdrawing functional groups such as NO₂ and CN on the aromatic ring, afford the highest efficiency. The ones with electron-donating provide biaryls in an acceptable yield but not as high as those with electron-withdrawing groups. And also, the phenylboronic acid bearing electron rich groups significantly facilitate the transmetallation step compared to those involving electron poor substituents. Therefore, a combination of aryl chlorides containing electron-withdrawing groups with phenylboronic acid involving electron-donating groups afforded desired biaryls with good yields (Table 2). On the other hand, considering the fact that heterobiaryls are of particular interest in the synthesis of natural products and the Suzuki cross-coupling reaction has been one of the synthetic methods, we explored the catalytic activity of the synthesized catalyst for the coupling of 4-chloropyridine and 2-chloropyridine with substituted phenylboronic acid. It was found that they are not efficient in these reactions and produce biaryls in much less yields because hetero-aromatic halides are generally less reactive than non-Heteroaryl halides due to the potential coordination of metal species with heteroatoms. Moreover, the electronic and steric properties are the other factor that decrease the yield of product as obtained for 1-(2'-methoxy-[1,1'-

biphenyl]-4-yl)ethanone.

3.3.3. Optimization of the reaction parameters for the Sonogashira cross-coupling reaction

The reaction of 1-chloro-4-nitrobenzene (1.0 mmol) and 1-ethynyl-4-methoxybenzene (1.2 mmol) was selected as a model reaction to optimized reaction parameters. The various parameters, including reaction temperature, type of base, solvent and amount of the catalyst were optimized (Table 3). Different amounts of the catalyst were examined and the best result was obtained by applying 6 mol% of the catalyst. No product was detected in the absence of the catalyst. The reaction was evaluated at different temperatures, and the highest yield obtained at 100 °C. Moreover, the model reaction was carried out with various types of bases, such as K₃PO₄, K₂CO₃, Na₂CO₃, Et₃N and NaHCO₃. On the basis of this study, K₂CO₃ showed the best performance. Subsequently, different solvents including PEG, DMSO, DMF and NMP were screened and finally PEG was chosen as the most effective solvent (Table 3).

3.3.4. Performance of the catalyst for the Sonogashira reaction

Encouraged by the achieved results from the Suzuki reaction, we then surveyed the generality of present catalyst toward the Sonogashira cross-coupling reaction. Under the optimal reaction condition. A diversity of aryl chlorides was used to react with substituted phenylacetylenes (Table 4). As exhibited in Table 4, the electronic variation of aryl chlorides smoothly affected the reaction efficiency. The aryl chlorides with electron-deficient groups such as cyano, nitro and acetyl participated in coupling process efficiently compared to those including electron-donating groups. It might be due to the decrease of electron density around aryl halide that makes it easy to dissociate the CX— bond and remove the halide from the substrate. Gratifyingly, the substituents on the para-, and meta-position of the phenylacetylenes slightly influence the activities. As evident from Table 4, phenylacetylene bearing methoxy and methyl substituents reacts effectively with aryl chlorides compared to its counterparts with acetyl substituent.

3.4. Recyclability of the catalyst

As an aspect of economic, environmental and industrial value, the recyclability of the catalyst was checked under the optimized conditions in the Suzuki and Sonogashira reactions as the model reaction. After completion of the reaction, the catalyst was separated by an external magnet, washed with ethanol and reused. As shown in Fig. S1, the catalyst was reused seven times without significant loss of activity. The reaction yield in the seventh runs decreased to 74 and 67 % for Suzuki and Sonogashira reactions, respectively.

In order to support this observation, the properties of the catalyst, including morphology, the amount of catalyst leaching and the presence of cobalt species were evaluated by TEM, FE-SEM, ICP-OES, and XRD techniques after seven runs (Fig. S2). As observed, the stability of the catalyst structure in the reaction mixture did not change and was similar to that of the fresh catalyst because no significant changes in the SEM and TEM images of the recycled catalyst were observed. Furthermore, Co-leaching determined by ICP-OES analysis reveals that less than 2% of cobalt metal was removed from the catalyst. As it is clearly seen, the XRD pattern of the reused catalyst and that of the fresh catalyst are similar and cobalt nanoparticles did not remove and were kept constant after seven runs.

3.5. Leaching test

Generally, the leaching test of metal nanoparticles was carried out after utilizing the catalyst in the coupling reaction. Therefore, the reaction between 1-chloro-4-nitrobenzene and (4-methoxyphenyl)boronic acid was performed under the optimized conditions. After half a minute, the reaction was stopped, and the catalyst was separated from the reaction media. Next, the reaction was continued without adding fresh

Table 4
Scope of the Sonogashira cross-coupling reaction in the presence of the synthesized catalyst^a.

^b Isolated yield.

^a The reaction was carried out with aryl halide (1.0 mmol), acetylene (1.2 mmol), K₂CO₃ (2 mmol), in 6 mL PEG, and catalyst (6 mol% of Co) at 100 °C.

catalyst under the same optimized conditions for 2 h. The progress of the reaction was assessed by GC and no further coupling reaction was observed. This result is proof for the heterogeneous nature of the catalyst and confirms the strong attachment of cobalt nanoparticles to the catalyst surface.

4. Conclusions

To summarize, Co-NHC@MC catalyst was successfully developed based on the immobilization of [mim]Cl backbone to magnetic chitosan nanoparticles and then coordination to cobalt species. High stability as well as catalytic activity of prepared catalyst toward readily available aryl chlorides substrates using 3 and 6 mol% of catalyst respectively for Suzuki and Sonogashira cross-coupling reactions, convinced us to result that the Co-NHC catalyst can be a good alternative catalyst to what is applied currently for Suzuki and Sonogashira coupling reactions. To the best of our knowledge, this is the first application of supported Co-NHCs for cross-coupling reaction of substituted phenylboronic acid and phenylacetylene with aryl chlorides. Additionally, the use of magnetically

separable metal catalyst, PEG as green solvent, mild conditions, recoverability up to 7 runs, and simple manipulations that require neither reducing agent nor cosolvent make this catalytic system an efficient catalyst for chemical reactions. Furthermore, the employment of Co-NHC@MC as a non-precious metal catalyst may be employed for other cross-coupling reactions that are in progress in our laboratory.

Declaration of Competing Interest

The authors declare that they have no known competing financial interests or personal relationships that could have appeared to influence the work reported in this paper.

Appendix A. Supplementary data

Supplementary material related to this article can be found, in the online version, at doi:<https://doi.org/10.1016/j.mcat.2021.111573>.

References

- [1] C.C. Johansson Seechurn, M.O. Kitching, T.J. Colacot, V. Snieckus, *Angew. Chem. Int. Ed.* 51 (2012) 5062–5085.
- [2] M.T. Chen, Y.H. Lin, K.H. Jian, *Appl. Organomet. Chem.* 34 (2020) 5955.
- [3] Y. Nishihara, E. Inoue, S. Noyori, D. Ogawa, Y. Okada, M. Iwasaki, K. Takagi, *Tetrahedron* 68 (2012) 4869–4881.
- [4] B. Jamwal, M. Kaur, H. Sharma, C. Khajuria, S. Paul, J. Clark, *New J. Chem.* 43 (2019) 4919–4928.
- [5] S. Rohani, A. Ziarati, G.M. Ziarani, A. Badieli, T. Burgi, *Catal. Sci. Technol.* 9 (2019) 3820–3827.
- [6] A. Maji, A. Singh, A. Mohanty, P.K. Maji, K. Ghosh, *Dalton Trans.* 48 (2019) 17083–17096.
- [7] R. KumaráBorah, H. JyotiáSaikia, V. KumaráDas, A. Jyotiá Thakur, *RSC Adv.* 5 (2015) 72453–72457.
- [8] T. Begum, M. Mondal, M.P. Borpuzari, R. Kar, G. Kalita, P.K. Gogoi, U. Bora, *Dalton Trans.* 46 (2017) 539–546.
- [9] Y. Dong, Y.Q. Chen, J.J. Jv, Y. Li, W.H. Li, Y.B. Dong, *RSC Adv.* 9 (2019) 21671–21678.
- [10] R. Bayan, N. Karak, *ACS Omega* 2 (2017) 8868–8876.
- [11] T. Ichikawa, M. Netsu, M. Mizuno, T. Mizusaki, Y. Takagi, Y. Sawama, Y. Monguchi, H. Sajiki, *Adv. Synth. Catal.* 359 (2017) 2269–2279.
- [12] T. Baran, *Carbohydr. Polym.* 195 (2018) 45–52.
- [13] S. Ostovar, A. Rezvani, R. Luque, C. Carrillo-Carrión, *Mol. Catal.* 493 (2020), 111042.
- [14] S. Elavarasan, K. Kala, I. Muhammad, A. Bhaumik, M. Sasidharan, *Mol. Catal.* 476 (2019), 110521.
- [15] A. Wolfson, O. Levy-Ontman, *Mol. Catal.* 493 (2020), 111048.
- [16] M. Arghan, N. Koukabi, E. Kolvari, *Appl. Organomet. Chem.* 33 (2019) e4823.
- [17] A. Guérinot, J. Cossy, *Acc. Chem. Res.* 53 (2020) 1351–1363.
- [18] J. Duczynski, A.N. Sobolev, S.A. Moggach, R. Dorta, S.G. Stewart, *Organometallics* 39 (2019) 105–115.
- [19] A.R. Hajipour, P. Abolfathi, Z. Tavangar-Rizi, *Appl. Organomet. Chem.* 32 (2018) e4353.
- [20] M.N. Hopkinson, C. Richter, M. Schedler, F. Glorius, *Nature* 510 (2014) 485–496.
- [21] K. Riener, S. Haslinger, A. Raba, M.P. Högerl, M. Cokoja, W.A. Herrmann, F. E. Kühn, *Chem. Rev.* 114 (2014) 5215–5272.
- [22] B. Heidari, M.M. Heravi, M.R. Nabid, R. Sedghi, *Appl. Organomet. Chem.* 33 (2019) 4934.
- [23] J.-H. Kim, J.-W. Kim, M. Shokouhimehr, Y.S. Lee, *J. Org. Chem.* 70 (2005) 6714–6720.
- [24] E. Niknam, F. Panahi, A. Khalafi-Nezhad, *Appl. Organomet. Chem.* 34 (2020) 5470.
- [25] M.-T. Chen, Z.-L. Kao, *Dalton Trans.* 46 (2017) 16394–16398.
- [26] Q.X. Liu, D.X. Zhao, H. Wu, Z.X. Zhao, S.Z. Lv, *Appl. Organomet. Chem.* 32 (2018) e4429.
- [27] V. Kandathil, A. Siddiqua, A. Patra, B. Kulkarni, M. Kempasiddaiah, B. Sasidhar, S. A. Patil, C.S. Rout, S.A. Patil, *Appl. Organomet. Chem.* 34 (2020) e5924.
- [28] T. Wang, J. Guo, X. Wang, H. Guo, D. Jia, H. Wang, L. Liu, *RSC Adv.* 9 (2019) 5738–5741.
- [29] T. Wang, H. Xie, L. Liu, W.-X. Zhao, *J. Organomet. Chem.* 804 (2016) 73–79.
- [30] T. Wang, L. Liu, K. Xu, H. Xie, H. Shen, W.X. Zhao, *RSC Adv.* 6 (2016) 100690–100695.
- [31] T. Wang, K. Xu, W. Wang, L. Liu, *Transit. Met. Chem.* 43 (2018) 347–353.
- [32] T. Wang, J. Guo, H. Wang, H. Guo, D. Jia, W. Zhang, L. Liu, *J. Organomet. Chem.* 877 (2018) 80–84.
- [33] A. Saroja, B.R. Bhat, *Ind. Eng. Chem. Res.* 58 (2018) 590–601.
- [34] A.R. Hajipour, F. Rezaei, Z. Khorsandi, *Green Chem.* 19 (2017) 1353–1361.
- [35] A.R. Hajipour, Z. Khorsandi, *Appl. Organomet. Chem.* 34 (2020) e5398.
- [36] M.A. Nasserli, Z. Rezazadeh, M. Kazemnejadi, A. Allahresani, *Dalton Trans.* 49 (2020) 10645–10660.
- [37] A. Mohammadinezhad, B. Akhlaghinia, *Green Chem.* 19 (2017) 5625–5641.
- [38] M. Arghan, N. Koukabi, E. Kolvari, *Appl. Organomet. Chem.* 33 (2019) 5075.
- [39] R.M. Jiménez-Barrera, V. Gómez-Benítez, M.G. Neira-Velázquez, J.R. Torres-Lubián, I. Moggio, E. Arias, R. Chan-Navarro, R. Guerrero-Santos, *Mol. Catal.* 464 (2019) 63–73.
- [40] M. Nasrollahzadeh, N. Motahharifar, F. Ghorbannezhad, N.S.S. Bidgoli, T. Baran, R.S. Varma, *Mol. Catal.* 480 (2020), 110645.
- [41] R. Zhong, A.C. Lindhorst, F.J. Groche, F.E. Kühn, *Chem. Rev.* 117 (2017) 1970–2058.
- [42] S.E. Hooshmand, B. Heidari, R. Sedghi, R.S. Varma, *Green Chem.* 21 (2019) 381–405.
- [43] H. Sharma, S. Sharma, C. Sharma, S. Paul, J.H. Clark, *Mol. Catal.* 469 (2019) 27–39.
- [44] Q. Zhang, X. Yang, J. Guan, *ACS Appl. Nano Mat.* 2 (2019) 4681–4697.
- [45] H. Veisi, T. Ozturk, B. Karmakar, T. Tamoradi, S. Hemmati, *Carbohydr. Polym.* 235 (2020), 115966.
- [46] N.Y. Baran, T. Baran, A. Menteş, *Carbohydr. Polym.* 181 (2018) 596–604.
- [47] T. Baran, M. Nasrollahzadeh, *Carbohydr. Polym.* 222 (2019), 115029.
- [48] A.S. Kritchenkov, A.V. Kletskov, A.R. Egorov, M.N. Kurasova, A.G. Tskhovrebov, V. N. Khrustalev, *Carbohydr. Polym.* 252 (2020), 117167.
- [49] C. Chen, *Phys. Chem. Liq.* 48 (2010) 298–306.
- [50] A.R. Hajipour, M. Check, Z. Khorsandi, *Appl. Organomet. Chem.* 31 (2017) e3769.
- [51] Y. Dong, X. Wu, X. Chen, Y. Wei, *Carbohydr. Polym.* 160 (2017) 106–114.
- [52] W. Wang, L. Cui, P. Sun, L. Shi, C. Yue, F. Li, *Chem. Rev.* 118 (2018) 9843–9929.
- [53] X. Cai, H. Wang, Q. Zhang, J. Tong, Z. Lei, *J. Mol. Catal. A: Chem.* 383 (2014) 217–224.
- [54] V.N. Khabashesku, J.L. Zimmerman, J.L. Margrave, *Chem. Mater.* 12 (2000) 3264–3270.
- [55] B. Huang, J. Chen, S. Zhan, J. Ye, *J. Electrochem. Soc.* 163 (2015) G26.
- [56] S. Rajendiran, K. Park, K. Lee, S. Yoon, *Inorg. Chem.* 56 (2017) 7270–7277.
- [57] P.R. Thombal, S.S. Han, *Biofuel Res. J.* 5 (2018) 886–893.
- [58] Z. Azarkamanzad, F. Farzaneh, M. Maghami, J. Simpson, *New J. Chem.* 43 (2019) 12020–12031.
- [59] S. Xuan, Y.X.J. Wang, J.C. Yu, K.C.F. Leung, *Langmuir* 25 (2009) 11835–11843.
- [60] S. Sobhani, H.H. Moghadam, J. Skibsted, J.M. Sansano, *Green Chem.* 22 (2020) 1353–1365.
- [61] H. Li, M. An, Y. Zhao, S. Pi, C. Li, W. Sun, H.g. Wang, *Appl. Surf. Sci.* 478 (2019) 560–566.